European Cells and Materials Vol.57 2026 (pages 199–210) DOI: 10.22203/eCM.v057a10 ISSN 1473-2262

Original Article

UTILIZATION OF CARTILAGE SHEETS FOR LOCALIZED TRACHEAL DEFECT REPAIR IN A GOAT MODEL

Ming Deng[1,§], Chao Wang[1,§], Yong Xu[1,*] and Gening Jiang[1,*]

[1]Department of Thoracic Surgery, Shanghai Pulmonary Hospital, Tongji University School of Medicine, 200433 Shanghai, China
[§]These authors contributed equally.

Abstract

Background: Repairing tracheal defects remains a significant challenge in tracheal surgery. Previous attempts using traditional tissue-engineered tracheal scaffolds in large animal models have largely failed due to inflammation and insufficient mechanical properties. **Methods:** In this study, we propose a novel approach that uses cell sheet technology to construct scaffold-free cartilage sheets *in vitro*. These sheets are stacked and then implanted into goats for further maturation, resulting in large neocartilage tissue with mechanical properties comparable to native tracheal cartilage. We evaluated three methods of tracheal defect repair in goat models using the stacked cartilage sheets: (1) In situ repair with stacked cartilage sheets without vascular pedicle; (2) In situ repair with stacked cartilage sheets and preservation of the vascular pedicle; (3) In situ repair with stacked cartilage sheets, preservation of the vascular pedicle, and T-tube insertion. **Results:** Airway stability was successfully restored in all animals, with all goats surviving until the end of the experiment without surgery-related complications. Goat 1 exhibited significant granulation tissue hyperplasia compared to goats 2 and 3. The airway morphology was best maintained in goat 3, which showed the highest degree of re-epithelialization, followed by moderate re-epithelialization in goat 2, and minimal in goat 1. **Conclusions:** These results suggest that stacked cartilage sheets are a viable option for tracheal repair, with vascular pedicle preservation and T-tube insertion enhancing therapeutic outcomes. Our study represents the first successful use of scaffold-free cartilage sheets for tracheal repair and provides a theoretical foundation for applying this technology in tracheal reconstruction.

Keywords: Cartilage sheet, scaffold free, tracheal repair, goat model, tissue engineering.

***Address for correspondence**: Yong Xu, Department of Thoracic Surgery, Shanghai Pulmonary Hospital, Tongji University School of Medicine, 200433 Shanghai, China. E-mail: xuyong@tongji.edu.cn; Gening Jiang, Department of Thoracic Surgery, Shanghai Pulmonary Hospital, Tongji University School of Medicine, 200433 Shanghai, China. E-mail: geningjiang@tongji.edu.cn.

Introduction

Airway structural damage or dysfunction can result from various factors [1]. For patients with localized tracheal defects, traditional segmental resection is technically challenging for large defects, involves significant trauma, and does not fully preserve the remaining healthy trachea [2]. Although several techniques have been proposed to reduce surgical trauma and preserve as much of the normal trachea as possible, these methods still cause substantial trauma at the donor site, and the outcomes are often inconsistent [3]. The use of biological patches for airway repair has been explored, but complete physiological reconstruction of the airway defect has not yet been achieved [4]. Thus, there is an urgent need to develop new treatment options.

Recent advances in tissue engineering offer promising solutions to this challenge [5,6]. The primary goal of tissue engineering is to create biologically functional living tracheal tissue for the permanent repair of tracheal defects. While tissue-engineered trachea has shown some success in reconstructing long tracheal defects in small animal models [7,8], these approaches often fail in larger animal models due to respiratory complications [9–11]. Large animal models, which better replicate human airway anatomy and physiology, are crucial for evaluating the efficacy of engineered tracheal substitutes [12]. Therefore, developing large animal models with closer anatomical and physiological similarity to humans is a key step in advancing tissue-engineered trachea reconstruction into clinical applications.

Tissue-engineered trachea protocols have achieved certain success in their application in small animal models (e.g., rabbits, mice), whereas attempts in large animal models have generally been unsuccessful. Traditional tissue-engineered tracheal repair strategies typically rely on scaf-

fold materials (biological or synthetic) as the core component [13]. Biological scaffolds, such as decellularized tissues, face challenges such as a lack of standardized decellularization protocols and difficulties in balancing immune compatibility with the preservation of native tissue mechanical properties [14–16]. Synthetic scaffolds, on the other hand, often induce immune responses due to degradation, impairing cartilage regeneration [17]. Despite efforts to mitigate these inflammatory responses [18–21], these solutions remain ineffective. As a result, scaffold-related challenges hinder the success of tissue engineering in large animal models, despite promising results in smaller ones.

In response to these challenges, cell sheet technology has emerged as a promising alternative [22]. Introduced in 1990, this technique has shown potential for regenerating various tissues [23,24]. Notably, cell sheet technology does not rely on external scaffold materials, potentially avoiding the immune-inflammatory responses associated with traditional scaffolds. Cartilage sheets produced through this method preserve cell-cell junctions and extracellular matrix (ECM) components, enabling the expression of genes and proteins related to cell adhesion and promoting cartilage formation [25,26]. By stacking multiple layers of cartilage sheets, their mechanical strength can be enhanced, making them suitable for meeting the mechanical demands of tissue-engineered trachea in large animal models [22].

To address these issues, we propose a novel strategy for preparing cartilage sheets *in vitro* using cell sheet technology. These stacked cartilage sheets will be implanted subcutaneously for further maturation. We will use these stacked cartilage sheets to repair tracheal window defects in a goat model, testing three approaches: 1) In situ tracheal repair using stacked cartilage sheets without vascular pedicle; 2) In situ tracheal repair using stacked cartilage sheets with vascular pedicle preservation; 3) In situ tracheal repair using stacked cartilage sheets without vascular pedicle, with T-tube insertion. Our study not only provides a new approach for treating tracheal window defects but also lays the theoretical groundwork for applying cell sheet technology to long-segment tracheal resection and reconstruction. We hope this research will advance clinical applications in tracheal surgery, transforming previously inoperable defects into operable ones, thereby simplifying procedures, reducing trauma, and offering promising clinical prospects.

Materials and Methods

Isolation of Primary Chondrocytes From Goat Auricular Cartilage

All animal procedures were carried out in adherence to the Guidelines for Care and Use of Laboratory Animals of Shanghai Pulmonary Hospital affiliated to Tongji University, and were approved by the Animal Ethics Committee of Shanghai Pulmonary Hospital affiliated to Tongji University. Six-month-old white goats (Shanghai Yunde Breeding Factory) were prepared, to induce anesthesia, goats received a single intramuscular injection of ketamine (5 mg/kg; Fujian Gutian Pharmaceutical Co., Ltd. China, H35020148), after which propofol (10 mL/min; Guangzhou Jiabo Pharmaceutical Co., Ltd. China, 191377109) was administered through intravenous infusion to maintain anesthesia. Endotracheal intubation was performed after adequate anesthesia, and mechanical ventilation was maintained via a ventilator. Approximately 5 × 6 cm sections of the auricle were excised under sterile conditions. The surface tissue was removed to expose the cartilage. The cartilage was pre-treated with 0.25% trypsin (Gibco, USA, 25200056) at 37°C for 30 minutes, then minced into approximately 1 mm^2 pieces. The minced cartilage was digested with 0.15% type II collagenase (Nordmark, Germany, S1745401) at 37°C, 100 rpm, for 12 hours. After digestion, the tissue was filtered through a 40 μm cell strainer (BD Falcon, USA, 352340) to remove residual fragments. The filtrate was centrifuged at 1500 rpm for 5 minutes, and the supernatant was discarded. The pellet was washed three times with phosphate-buffered saline (PBS, Gibco, USA, 10010023) and centrifuged again to collect the primary chondrocytes.

Primary Culture and Passage Expansion of Chondrocytes

The isolated primary chondrocytes were resuspended in Dulbecco's modified Eagle medium (DMEM, Gibco, USA, 11995065) containing 10% fetal bovine serum (FBS, Gibco, USA, 16000-044) and 1% penicillin–streptomycin (Gibco, USA, 15140-122). Cell viability was assessed using Trypan Blue staining (Beyotime, China, ST798). Chondrocytes were plated at a density of 2 × 10^6 cells per 100 mm culture dish (Corning, USA, 430167) and cultured in a humidified incubator at 37°C with 5% CO_2. The medium was replaced every 2–3 days. Once the chondrocytes reached 90% confluence, they were passaged at a 1:4 ratio into new 100 mm plates and cultured under the same conditions.

In Vitro Formation of Cartilage Sheets

Passage 2 (P2) chondrocytes were digested, centrifuged, and resuspended in complete medium. The cells were plated at 5 × 10^6 cells/cm^2 in 6-well plates (Corning, USA, 3516) and induced with DMEM supplemented with 10 ng/mL transforming growth factor beta1 (R&D Systems, MN, USA, 7754-BH-025), 50 ng/mL insulin-like growth factor-I (R&D Systems, MN, USA, 291-G1-200), insulin-transferrin-selenium-X (Gibco, USA, 51500056), and ascorbic acid (Sigma, USA, A4544) at 37°C in a 5% CO_2 incubator. The cartilage sheets were cultured for 8 weeks. Samples were carefully peeled off the plates using forceps and analyzed at the 2nd, 4th, and 8th weeks.

In Vivo Culture of Stacked Cartilage Sheets

The anesthesia procedure was consistent with that described above, after anesthesia, a 4 cm longitudinal incision was made along the midline of the goat's neck, and a skin flap was raised to form a pouch. Two pieces of cartilage sheets were stacked and implanted into the pouch. The incision was sutured intermittently. From the day of surgery, goats received intramuscular penicillin (Huachu, China, 1292) for 3 days. Samples were collected for histological analysis at the 4th and 8th weeks.

In Situ Tracheal Repair Using Stacked Cartilage Sheets

After 8 weeks of *in vivo* implantation, goats were anesthetized, and a 4 cm longitudinal incision was made along the midline of the neck. Subcutaneous tissue and pre-tracheal muscles were dissected layer by layer to expose the cervical trachea. A 1.5 × 2 cm segment of tracheal cartilage was excised. A second incision was made on the opposite side of the neck to fully expose the stacked cartilage sheet. The sheet was trimmed to fit the defect. Three goats were divided into three treatments using the random sampling method; in situ tracheal repairs were performed as follows:

Treatment 1 (No vascular pedicle; goat 1): The stacked cartilage sheet was fully dissociated and sutured onto the tracheal defect using 4-0 polysorb (Covidien, USA, UL203) sutures.

Treatment 2 (Vascular pedicle preservation; goat 2): The stacked cartilage sheet was partially dissociated, preserving a unilateral vascular pedicle, and sutured onto the defect using 4-0 polysorb sutures.

Treatment 3 (No vascular pedicle + T-tube insertion; goat 3): The stacked cartilage sheet was fully dissociated without a vascular pedicle. A T-tube was inserted through a cut in the trachea, extending 1 cm beyond the defect, and the sheet was sutured using 4-0 polysorb sutures.

The surrounding neck muscles were freed and sutured to cover the cartilage sheet and surrounding tissues. The incision was closed in layers. The goats were treated with penicillin for 7 days, and respiratory condition and weight changes were monitored. After 6 months, euthanasia was performed, and tissue samples from the repair site and adjacent native trachea were collected.

Relevant Testing of Cartilage Sheets

Cartilage sheet samples were collected at the 2nd, 4th, and 8th weeks of *in vitro* culture, and at the 4th and 8th weeks of *in vivo* culture. Histological analyses, including Hematoxylin and Eosin (H&E) staining (Proteintech, China, PK10031), Safranin-O staining (Solarbio, China, G1371), Masson's trichrome staining (Solarbio, China, G1340), and immunohistochemistry/immunofluorescence staining for type II collagen (COL II, Proteintech, China, 28459-1-AP/CL488-28459) were performed. Quantitative analyses included measurements of DNA content, glycosaminoglycan (GAG) content, and COL II content following methods described in prior reports [17]. The GAG/DNA and COL II/DNA ratios were determined based on the collected data.

The thickness was measured from H&E sections, to ensure consistency and representativeness, all measurements were systematically taken from the central, flattest region of each construct, avoiding the rolled edges.

The wet weight of the regenerated cartilage was measured immediately after retrieval. Each construct was briefly rinsed with PBS to remove culture medium, gently blotted on filter paper to remove excess surface moisture, and then weighed on a microbalance.

The Young's modulus of all samples was determined using a biomechanical analyzer (Instron-5542, Canton, USA) with a constant crosshead speed of 1 mm/min, following a previously established method [16]. The samples, which included *in vitro*-cultivated cartilage sheets (2, 4, 8 weeks), *in vivo*-cultivated stacked sheets (4, 8 weeks), and native tracheal cartilage (n = 3 per group), were subjected to unconfined compression up to 80% of their maximal deformation. The modulus was calculated from the slope of the resulting stress-strain curve.

Additionally, tracheal samples from all goats (1, 2, and 3) were collected from areas where the stacked cartilage sheets were located, as well as from adjacent tracheal segments. These samples were subjected to gross observation and histological analysis using H&E, Safranin-O, Masson's trichrome staining, and immunohistochemical COL II staining.

Statistical Methods

Data were analyzed using SPSS 26 software (IBM Corp., Armonk, NY, USA). Quantitative data are presented as means ± standard deviation. A T-test was used for intergroup comparisons, and differences were considered statistically significant when $p < 0.05$.

Results

In Vitro Formation of Cartilage Sheets

Upon seeding primary chondrocytes at a density of 2×10^6 cells per 100 mm culture dish, light microscopic observations revealed rapid expansion from day 0 to day 4. After adhering to the surface, they adopted a polygonal shape (Fig. 1**a**).

To obtain sufficient chondrocytes for subsequent cartilage sheet formation, the primary chondrocytes were passaged to P2. The P2 chondrocytes proliferated rapidly and achieved confluence by day 4 (Fig. 1**b**), indicating their favorable viability. Given that P2 chondrocytes maintained a similar phenotype to primary chondrocytes, they were selected for the preparation of cartilage sheets in subsequent experiments.

The P2 chondrocyte suspension was seeded at a density of 5×10^6 cells/cm^2 in 6-well plates. After 4 days of

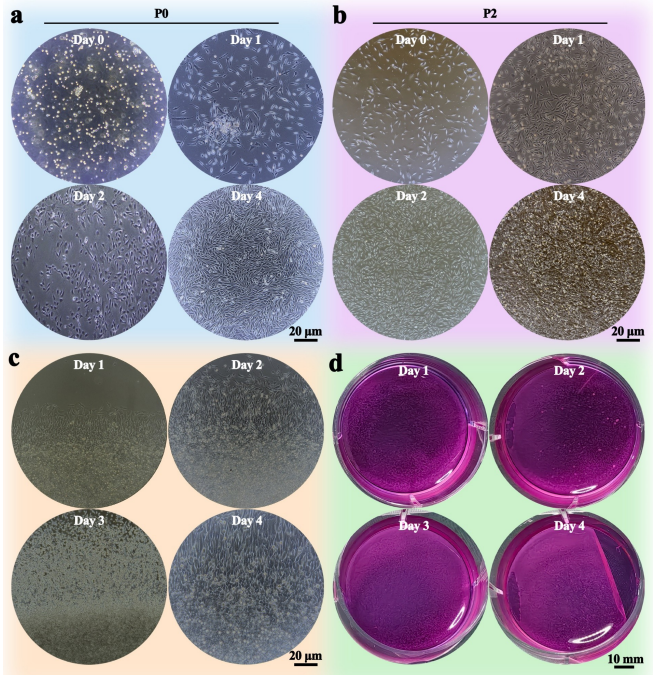

Fig. 1. *In vitro* cultivation of chondrocytes and formation of primary cartilage sheets. (**a**) Light microscopy images of primary chondrocyte culture from day 0 to day 4. (**b**) Light microscopy images of P2 chondrocyte culture from day 0 to day 4. (**c**) Light microscopy images showing the development of cartilage sheets from day 1 to day 4 of culture. (**d**) Macroscopic images of cartilage sheets from day 1 to day 4 of culture.

culture, the chondrocytes at the plate edges were fully integrated, expanding outward to fill the entire well, showing signs of overlay fusion (Fig. 1**c**). At day 4, the chondrocytes began to form a stacked, three-dimensional structure, making individual cells difficult to distinguish under the microscope.

Macroscopic observation revealed a thin, translucent cartilage sheet at the bottom of the culture dish by day 1. As the culture progressed, the sheet thickened, transitioning from translucent to opaque white and gelatinous between days 1 and 4 (Fig. 1**d**). However, the sheet was still too weak to handle at day 4.

Therefore, we extended the *in vitro* chondrogenic culture to 8 weeks. Over time, the cartilage sheet thickened and gradually changed from translucent to milky white (Fig. 2**a**). By the 8th week, the cartilage sheet had matured with a uniform, smooth surface and a semi-translucent, milky appearance. The sheet could be easily peeled from the culture plates using forceps.

Histological analysis revealed that the thickness and cartilage-specific ECM secretion of the cartilage sheets increased gradually. Lacunae-like structures began to form, consistent with macroscopic observations. By the 8th week, the sheets had a porcelain white appearance with increased thickness and clear ECM deposition, as confirmed by H&E, Safranin-O, and immunofluorescence COL II staining (Fig. 2**b**–**d**). This finding was further confirmed by immunofluorescence staining of COL X and MMP-13 (**Supplementary Fig. 1**).

Quantitative analysis demonstrated steady improvements in Young's modulus (Fig. 2**e**), thickness (Fig. 2**f**), wet weight (Fig. 2**g**), DNA content (Fig. 2**h**), GAG/DNA ratio (Fig. 2**i**), and COL II/DNA ratio (Fig. 2**j**) over the culture period. These results suggest that chondrocytes gradually matured into cartilage tissue during the *in vitro* culture process.

In Vivo Formation of Stacked Cartilage Sheets

Given that the thickness and mechanical properties of a single cartilage sheet were insufficient for tracheal repair, two cartilage sheets were stacked and implanted subcutaneously in goats to generate a more robust graft.

A 4 cm longitudinal incision was made along the midline of the goat's neck (Fig. 3**a**), and a skin flap was raised to form a pouch (Fig. 3**b**). The stacked cartilage sheets were placed into the pouch (Fig. 3**c**–**e**), and the incision was sutured intermittently (Fig. 3**f**).

Macroscopic observations revealed that, after 4 weeks, the stacked cartilage sheets had a red appearance with an uneven surface. However, after 8 weeks of *in vivo* culture, they appeared porcelain white with a smooth surface, showing improved cartilage-like features compared to those at 4 weeks (Fig. 3**g**).

Histological examination using H&E staining revealed that the chondrocytes within the stacked cartilage sheets maintained normal morphology and staining, with lacunae-like structures surrounding the chondrocytes, resembling native cartilage. At 8 weeks, the cartilage sheets

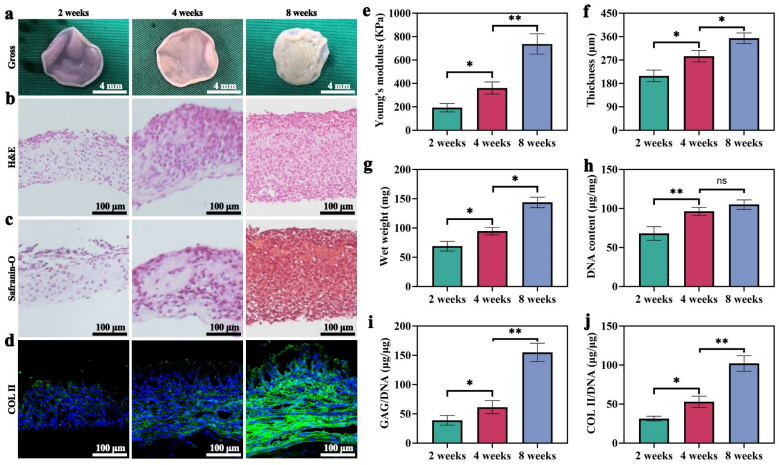

Fig. 2. Prolonged *in vitro* cultivation of cartilage sheets. (**a**) Macroscopic observation of cartilage sheets at weeks 2, 4, and 8 of *in vitro* culture. (**b**) H&E staining of cartilage sheets at weeks 2, 4, and 8 of *in vitro* culture. (**c**) Safranin-O staining of cartilage sheets at weeks 2, 4, and 8 of *in vitro* culture. (**d**) COL II immunofluorescence staining of cartilage sheets at weeks 2, 4, and 8 of *in vitro* culture. (**e**) Comparison of Young's modulus, (**f**) thickness, (**g**) wet weight, (**h**) DNA content, (**i**) GAG/DNA ratio, and (**j**) COL II/DNA ratio of cartilage sheets at weeks 2, 4, and 8 of *in vitro* culture. $^{*}p < 0.05$; $^{**}p < 0.01$. ns, no significance. n = 3.

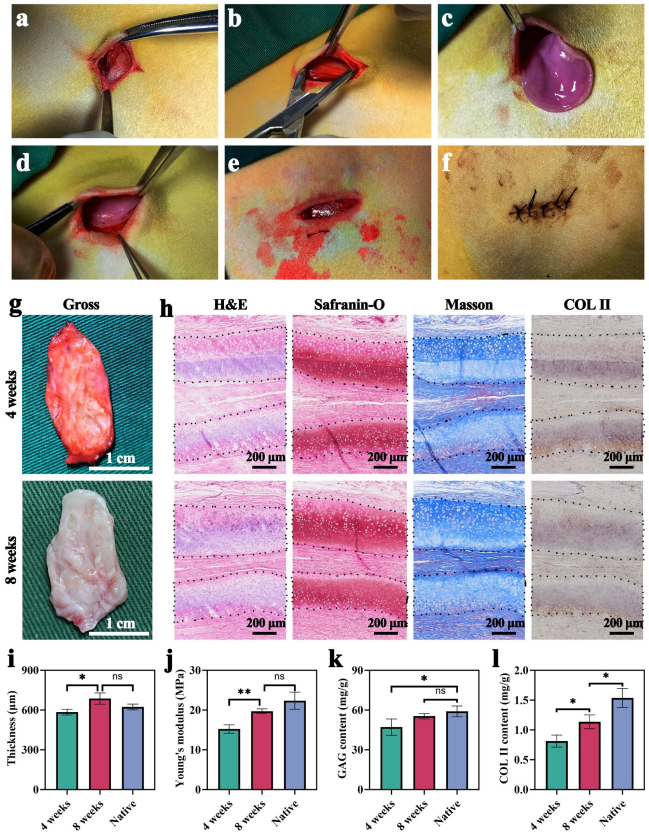

Fig. 3. *In vivo* cultivation of stacked cartilage sheets. (**a**) A 4 cm longitudinal incision was made at the midline of the goat's neck. (**b**) A skin flap was raised to form a pouch. (**c-e**) The layered cartilage sheets were placed into the pouch. (**f**) The incision was intermittently sutured. (**g**) Macroscopic observation of cartilage sheets at weeks 4 and 8 of *in vivo* culture. (**h**) Histological analysis of cartilage sheets at weeks 4 and 8: H&E staining, Safranin-O staining, Masson's Trichrome staining, and COL II immunohistochemical staining (Black dashed lines labeled the regenerated cartilage sheet layers). (**i**) Comparison of thickness, (**j**) Young's modulus, (**k**) GAG/DNA ratio, and (**l**) COL II/DNA ratio of cartilage sheets at weeks 4 and 8 of *in vivo* culture and native tracheal cartilage. $^{*}p < 0.05$; $^{**}p < 0.01$. ns, no significance. n = 3.

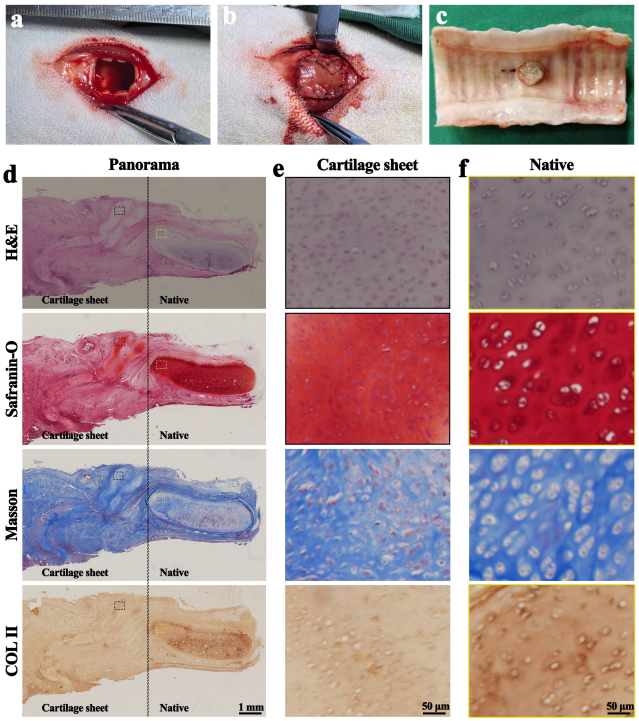

Fig. 4. In situ tracheal repair using stacked cartilage sheets without a vascular pedicle. (**a**) Creation of the tracheal window defect. (**b**) Repair of the tracheal defect using a cartilage sheet without a vascular pedicle. (**c**) Macroscopic observation of the repair area 6 months post-surgery. (**d**) Longitudinal sections showing the repaired area, stained with H&E, Safranin-O, Masson's Trichrome, and immunohistochemical COL II staining. (**e**) Magnified images of the cartilage sheet from the area indicated by the black dotted square in panel (**d**). (**f**) Magnified images of the native trachea from the area indicated by the yellow dotted square in panel (**d**). The black dotted line indicates the border between the repair area and the native trachea.

were thicker than at 4 weeks, with more prominent lacunae and a more uniform interior. Safranin-O staining, Masson's Trichrome staining, and immunohistochemical COL II staining confirmed the deposition of cartilage-specific ECM, such as GAG and COL II (Fig. 3**h**).

Notably, fibrous tissue began to grow between the layers of the stacked cartilage sheets. Histological staining revealed stratification within the single-layer cartilage sheets after 4 weeks, with the stratified tissue consisting of cartilage. By week 8, the internal structure of the stacked sheets had become more uniform, and muscle tissue had begun infiltrating the cartilage sheet on the muscle side, where COL II deposition was more prominent (Fig. 3**h**). This finding was further confirmed by immunofluorescence staining of COL X and MMP-13 (**Supplementary Fig. 2**).

Quantitative analysis indicated that the stacked cartilage sheets' thickness (Fig. 3**i**), Young's modulus (Fig. 3**j**), and GAG deposition (Fig. 3**k**) increased to levels comparable to or exceeding natural tracheal cartilage. While COL II deposition had not yet matched the levels of native tracheal cartilage at 8 weeks, it increased steadily during *in vivo* culture (Fig. 3**l**). These results suggest that the stacked cartilage sheets matured over time, achieving mechanical properties, ECM deposition, and thickness similar to native tracheal cartilage.

In Situ Tracheal Repair via Stacked Cartilage Sheet Without Vascular Pedicle

A tracheal cartilage patch was excised from the anterior trachea (Fig. 4**a**), and the *in vivo* obtained cartilage sheet without a vascular pedicle was sutured onto the tracheal defect (Fig. 4**b**). At 6 months post-surgery, the goats remained healthy, with normal eating, breathing, and vocalization, and stable weight gain. No anastomotic complications or respiratory infections were observed, and no life-threatening events occurred. The stability of the repaired trachea was acceptable, with approximately 50% lumen narrowing. A spherical mass of granulation tissue was observed in the central repair area, surrounded by a smooth inner tracheal wall (Fig. 4**c**).

Histological examination revealed native tracheal cartilage and the cartilage graft. The proximal part of the graft maintained its morphology well, with ECM deposition approaching that of native tracheal cartilage (Fig. 4**d**–**f**). Cartilage phenotype was preserved by these patches in all three goats postoperatively (**Supplementary Fig. 3**).

In Situ Tracheal Repair via Stacked Cartilage Sheet With Vascular Pedicle Preservation

A tracheal cartilage patch was excised from the anterior trachea (Fig. 5**a**), and the stacked cartilage sheet

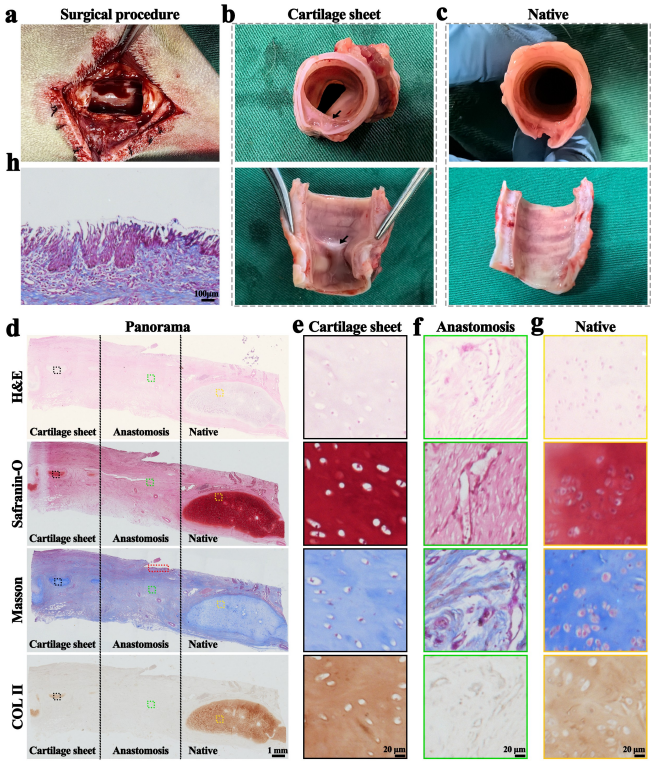

Fig. 5. In situ tracheal repair using stacked cartilage sheets with vascular pedicle preservation. (**a**) Creation of the tracheal window defect. (**b**) Macroscopic observation of the trachea at 6 months post-surgery, with the repair area indicated by black arrows. (**c**) Macroscopic observation of the native trachea. (**d**) Longitudinal sections of the repaired area, stained with H&E, Safranin-O, Masson's Trichrome, and COL II immunohistochemical staining. (**e**) Magnified images of the cartilage sheet from the area indicated by the black dotted square in panel (**d**). (**f**) Magnified images of the anastomosis area from the area indicated by the green dotted square in panel (**d**). (**g**) Magnified images of the native trachea from the area indicated by the yellow dotted square in panel (**d**). (**h**) Tracheal epithelium in the repaired area within the cartilage sheet, as indicated by the red dotted square in panel (**d**). Black dotted lines indicate the borders between the repair area, anastomosis area, and native trachea.

with vascular pedicle preservation was sutured onto the tracheal defect. At 6 months post-surgery, the goats were healthy with normal physiological functions. The tracheal repair showed approximately 40% lumen narrowing, with a smooth, milky-white repair area and no significant granulation tissue proliferation (Fig. 5**b**). The repair area closely resembled the native trachea (Fig. 5**c**).

Histological analysis revealed partial resorption of the cartilage graft, and both GAG and COL II deposition reached levels comparable to native tracheal cartilage (Fig. 5**d**–**g**). Moderate re-epithelialization was observed, with the airway epithelium migrating into the graft area; however, extensive coverage had not yet occurred (Fig. 5**h**).

In Situ Tracheal Repair via Stacked Cartilage Sheet Without Vascular Pedicle and T-Tube Insertion

A tracheal cartilage patch was excised from the anterior trachea, and the stacked cartilage sheet without a vascular pedicle was sutured to the tracheal defect (Fig. 6**a**). At 6 months post-surgery, the goats remained healthy with no anastomotic complications or signs of infection. The repaired trachea showed no significant narrowing or softening (Fig. 6**b**–**c**). A small amount of granulation tissue growth was observed in the lumen, and the surrounding mucosa remained smooth (Fig. 6**d**).

Histological analysis showed native tracheal cartilage and the repaired graft, with the proximal part of the graft maintaining its morphology well. ECM deposition in the graft reached levels comparable to native tracheal cartilage. However, partial cartilage destruction, inflammatory cell infiltration, and partial resorption were observed in the central region (Fig. 6**e**–**g**). Notably, extensive re-epithelialization was observed in the central region, with airway epithelium migrating into the graft (Fig. 6**h**).

Discussion

Tracheal reconstruction remains a significant challenge in tracheal surgery [27]. While tissue-engineered tracheal substitutes have shown intermediate-term success in small animal models for treating tracheal defects [28], attempts to reconstruct large-scale defects in large animal models have generally failed, with only limited success reported by a few groups [11,29]. In this study, we propose using cell sheet technology to create scaffold-free cartilage

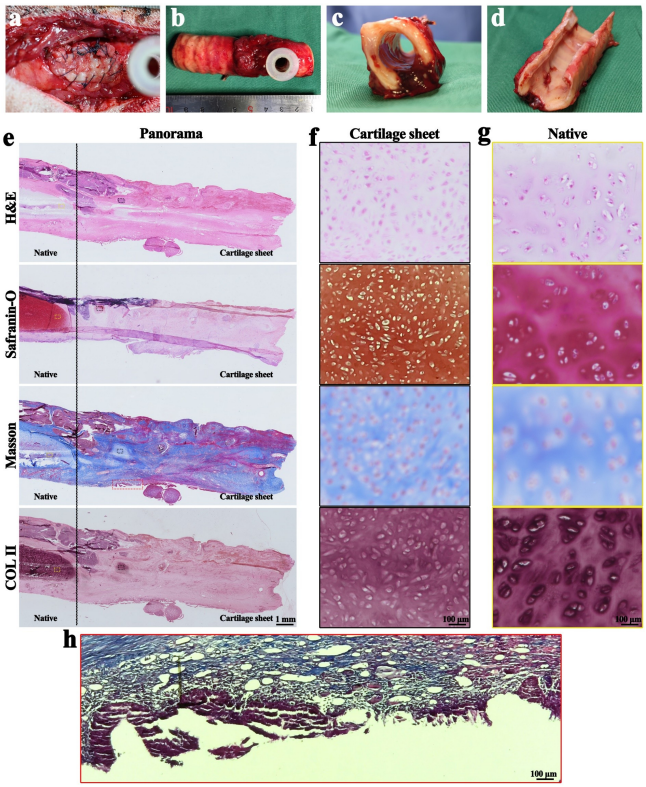

Fig. 6. In situ tracheal repair using stacked cartilage sheets without vascular pedicle and T-tube insertion. (**a**) Repair of the tracheal defect using a cartilage sheet without a vascular pedicle and with T-tube insertion. (**b**–**d**) Macroscopic observation of the trachea at 6 months post-surgery, showing multiple views of the repair area. (**e**) Longitudinal sections of the repaired area, stained with H&E, Safranin-O, Masson's Trichrome, and COL II immunohistochemical staining. The black dotted line indicates the border between the repair area and native trachea. (**f**) Magnified images of the cartilage sheet from the area indicated by the black dotted square in panel (**e**). (**g**) Magnified images of the native trachea from the area indicated by the yellow dotted square in panel (**e**). (**h**) Tracheal epithelium in the repaired area within the cartilage sheet, as indicated by the red dotted square in panel (**e**).

sheets *in vitro*, which, after *in vivo* maturation, can repair tracheal window defects in large animal models.

We successfully developed cartilage sheets *in vitro*. During culture, the sheet thickness gradually increased, and both the mechanical properties and deposition of cartilage-specific ECM components improved. ECM deposition accelerated significantly over the course of 8 weeks, which correlated with the increase in Young's modulus measured during testing. In the first four weeks, DNA quantification revealed vigorous cell proliferation, with cell division outpacing ECM secretion. During this period, the deposition of GAGs and COL II steadily increased, and mechanical properties also improved. After the fourth week, cell proliferation slowed, and ECM secretion became more prominent. This resulted in accelerated deposition of cartilage-specific ECM components and a marked improvement in the mechanical properties of the cartilage sheets.

In the *in vivo* phase, we overlapped two cartilage sheets before implantation to further enhance their mechanical properties. In both 4-week and 8-week samples, we observed vascularized fibrous connective tissue growing between the overlapping sheets, which may improve blood supply to the cartilage. Histological examination of the 4-week samples revealed uneven development within the cartilage sheet, possibly due to variability in blood supply or differences in the central and peripheral areas of the graft. By the 8th week, histology showed significant improvement, with better overall uniformity, indicating that longer *in vitro* culture promotes maturation of the cartilage sheets and partially compensates for earlier limitations. After 8 weeks of *in vivo* implantation, the stacked cartilage sheets reached thickness, mechanical properties, and ECM deposition levels comparable to native tracheal cartilage. Importantly, after implantation into goats, the stacked cartilage sheets remained stable, with no signs of disintegration or immune rejection. This approach avoids the use of scaffold materials, thereby minimizing the risk of scaffold-related inflammatory responses and achieving *in vivo* regeneration of tissue-engineered cartilage.

This study emphasizes the role of stacked cartilage sheets in restoring airway stability. In our large animal model, the stacked cartilage sheets successfully repaired the airway defect, ensuring stable survival for 6 months without any additional intervention. In goats 1 and 2, normal

tracheal cartilage on both sides of the repair site migrated toward the center, resulting in airway stenosis. However, in goat 3, no such phenomenon was observed, suggesting that early placement of a T-tube helps maintain normal airway morphology before the patch fully integrates [30]. Despite these differences in morphology, no adverse events such as airway collapse occurred in any goat, and the airway morphology remained stable with mechanical properties similar to normal tracheal segments. After the T-tube removal, airway morphology remained stable in goat 3, and the mechanical properties were good. These results suggest that stacked cartilage sheets can restore airway defect morphology, and that previous failures in tracheal reconstruction using cartilage patches may not be due to the inherent properties of the patches themselves. Our data support the feasibility of using stacked cartilage sheets as tracheal substitutes for large animal models of airway defect repair.

The airway epithelium plays a crucial role in maintaining the airway barrier and assisting in the clearance of airway secretions [31]. However, pre-constructing a functional airway epithelium remains challenging, as previous studies often failed to achieve complete epithelialization of tracheal grafts or replaced the epithelium with squamous epithelial tissue [17,22]. Some studies suggest that the absence of certain epithelial functions can be compensated by the cough reflex [22,32,33] and that the airway epithelium has limited migratory capacity [34]. Preclinical study has indicated re-epithelialization occurs from migration of cells from the wound edge [35], And re-epithelialization of tracheal grafts has also been observed in some case reports [34,36]. But the destiny of such epithelium is hard to be observed *in vivo* due to the lack of a safe and reliable approach. In long-segment tracheal transplants, limited epithelial migration often prevents complete epithelialization of the graft. However, in tracheal window defects, the smaller graft area may facilitate more effective epithelialization. In our study, the airway epithelium migrated from the peripheral area of the patch to the central region. In contrast to long-segment tracheal replacements, the smaller repair area required for tracheal window defects theoretically may reduce the difficulty of re-epithelialization via natural epithelial migration. Our results showed that, except in goat 1, where significant granulation tissue proliferation occurred, goats 2 and 3 exhibited clear epithelial migration, with granulation tissue proliferation within acceptable limits and no adverse events such as airway stenosis caused by excessive granulation tissue [37]. No significant mucus accumulation was observed in the harvested tracheal specimens [11]. This study demonstrates that, in small-area tracheal replacements, stacked cartilage sheets can achieve good re-epithelialization through migration of surrounding normal tracheal epithelium without severe granulation tissue proliferation or other adverse events. Similarly, we are unable to determine the occurrence, development, and ultimate fate of this epithelium for the time being.

The unique vascular supply pattern of the trachea makes achieving vascularization of tracheal substitutes via conventional vascular anastomosis particularly challenging [38]. Autologous tissue wrapping is often used for indirect vascularization, but this requires a second surgery and results in significant trauma. While the muscle-attachment vascular reconstruction model proposed by Delaere *et al*. [39] successfully maintains the vitality of tracheal cartilage, ischemic necrosis of the tracheal epithelium still occurs, suggesting that mature cartilage has lower metabolic demands. In our study, the cartilage sheet exhibited good vascular reconstruction. Inspired by Delaere *et al*. [39] 's work, we hypothesized that attachment of unilateral muscle tissue would suffice to sustain the normal metabolism of small cartilage pieces. Our results showed significant vascularization around the cartilage patch. There was no significant difference in inflammatory cell infiltration between the preserved blood supply goat (goat 2) and the reconstructed blood supply goats (goats 1 and 3). However, the preserved blood supply goat demonstrated better protection of cartilage tissue in the central region of the sheets, with less granulation tissue proliferation compared to the reconstructed blood supply goat. This approach simplified the surgical procedure and avoided damage to the donor site.

Postoperative inflammation cannot be completely avoided. Histological analysis showed that in the reconstructed blood supply goat, inflammatory cell infiltration was concentrated in the central region of the cartilage sheet, which was also the area of most cartilage resorption. In contrast, cartilage preservation was better at the anastomotic site and in areas further from the airway lumen. We speculate that cartilage resorption in the central region of the sheet may due to two factors: (1) The central region's blood supply took longer to reconstruct, as the peripheral region received blood from both the anastomosis and overlying muscle, while the central region only received blood from the overlying muscle, resulting in relative ischemia; and (2) epithelial reconstruction in the central region was slower. Since we did not pre-implant epithelial tissue within the stacked cartilage sheets, the central region was the last to be protected by the airway epithelium, potentially leading to local infection and inflammation. These factors likely contributed to the persistent inflammatory response and cartilage resorption in the central region. Despite partial cartilage resorption, mechanical properties did not significantly decrease, and all experimental goats showed stable airway morphology, capable of withstanding external pressure.

We note that in Makris *et al*. [40] 's study, similar inflammatory responses and tissue resorption were observed early postoperatively. However, with extended postoperative time, histological analysis revealed neogenesis of cartilage tissue. Given the lack of longer-term data, we cannot yet determine the outcome of using stacked cartilage sheets for tracheal defect repair.

The traditional view holds that chondrocytes are encapsulated within the cartilage matrix and are nourished through the diffusion of nutrients from extra-cartilaginous capillaries. The dense collagen matrix can prevent antigens from being recognized by the recipient's immune cells or entering the recipient's lymphoid tissues, thus endowing a certain degree of immune privilege [41,42]. Previous cases of allogeneic tracheal transplantation have indicated that after discontinuing immunosuppression, the mechanical support strength provided by the graft remains unchanged [36]. A similar phenomenon has also been observed in animal experiments [43,44], which confirms the protection of tracheal cartilage from immune recognition and destruction. Of course, as an organ with a complex organizational structure, the trachea requires in-depth research on the host immune response during its transplantation and reconstruction process. This is an important future research direction and also one of the focuses of our future work.

Our approach has some limitations. First, the number of chondrocytes required is relatively large, and for larger reconstructions, more cartilage tissue may need to be harvested, or an alternative source of chondrocytes may be necessary [45]. Autologous stem cell recruitment is also a promising direction [46]. Second, the overall construction cycle for our approach is longer, and experimental costs are higher. Additionally, our *in vitro* cartilage sheets method involves planar culture, which may lead to differences in energy access, cytokine concentration, and metabolic waste accumulation between the surface and bottom layers of chondrocytes as the sheets become thicker [47]. Although the use of an internal airway scaffold could raise concerns about scaffold-related complications [48], our T-tube design did not cause such issues. Future work should explore alternative scaffold designs, such as pure lumen scaffolds with specialized surface coatings or fully absorbable scaffolds, to further minimize graft-related injury [49]. Finally, the small sample size in this study, due to differences in animal management, surgical support, postoperative care, and funding, limits the ability to conduct large-scale, long-term experiments, making it difficult to effectively eliminate the interference of random factors like individual variations and surgical operation discrepancies on the results. Admittedly, the small sample size does impose certain limitations on the generalizability of the findings. However, our study was designed as a small-scale proof-of-concept; the key significance of this research lies in "first verifying the feasibility of using scaffold-free cartilage sheets to repair tracheal defects in large animals", thus laying a methodological foundation for subsequent large-scale studies. We believe that the limitations can be gradually overcome by increasing the sample size and optimizing the experimental design in future work. Furthermore, we euthanized the goats at 6 months post-surgery to obtain tracheal specimens, limiting our ability to track early and long-term postoperative healing. We will expand the sample size and use this technique to repair circumferential tracheal defects in goat models in further work.

Conclusions

We have proposed a novel approach for repairing tracheal window defects in large animal models using scaffold-free cartilage sheets created with cell sheet technology. The use of stacked cartilage sheets successfully restored airway integrity and stability, allowing for long-term survival of the animals without fatal complications. Airway stability was effectively reconstructed in all three experimental goats, with goat 3 showing the best maintenance of airway morphology and the highest degree of re-epithelialization. This study represents the first attempt to apply a scaffold-free tissue engineering approach to tracheal repair, establishing a theoretical foundation for using cell sheet technology in long-segment tracheal resection and reconstruction. Our findings offer potential for converting non-resectable tracheal lesions into resectable ones, simplifying complex surgeries, and holding promising clinical applications in tracheal surgery.

Availability of Data and Materials

The data that support the findings of this study are available from the corresponding authors upon reasonable request.

Author Contributions

GNJ, YX conceived the study design and critically revised the manuscript for key intellectual content; MD, CW performed data interpretation and analysis, and drafted the original manuscript. All authors read and approved the final manuscript. All authors agree to be accountable for all aspects of the work in ensuring that questions related to the accuracy or integrity of any part of the work are appropriately investigated and resolved.

Ethics Approval and Consent to Participate

The research protocol was approved by the Ethics Committee of Shanghai Pulmonary Hospital affiliated to Tongji University (NO. K23-170Y).

Acknowledgments

We gratefully acknowledge the assistance and instruction from Dr. PengLi Wang of Tongji University for specimen preparation.

Funding

This work is sponsored by the Natural Science Foundation of Shanghai (22Y21900700), and the National Natural Science Foundation of China (82302395).

Conflict of Interest

The authors declare no conflict of interest.

Supplementary Material

Supplementary material associated with this article can be found, in the online version, at https://doi.org/10.22203/eCM.v057a10.

References

[1] Genden EM, Laitman BM. Human Tracheal Transplantation. Transplantation. 2023; 107: 1698–1705. https://doi.org/10.1097/tp.0000000000004509.

[2] Shan Y, Shen Z, Lu Y, Zhu J, Sun F, Chen W, *et al*. Reconstruction of tracheal window-shape defect by 3D printed polycaprolatone scaffold coated with Silk Fibroin Methacryloyl. Biotechnology Journal. 2024; 19: e2300040. https://doi.org/10.1002/biot.202300040.

[3] Delaere P, Meulemans J, Vranckx J, Vos R, Poorten VV. Tracheal Transplantation. Thoracic Surgery Clinics. 2025; 35: 131–141. https://doi.org/10.1016/j.thorsurg.2024.07.002.

[4] Lu CW, Liao HC, Tsou KC, Hung WT, Huang PM, Hsu HH, *et al*. Cryopreserved aortic graft patch repair of traumatic tracheal rupture defect: A case report. JTCVS Techniques. 2024; 27: 182–184. https://doi.org/10.1016/j.xjtc.2024.07.023.

[5] Yang Y, Zhu X, Liu X, Chen K, Hu Y, Liu P, *et al*. Injectable and self-healing sulfated hyaluronic acid/gelatin hydrogel as dual drug delivery system for circumferential tracheal repair. International Journal of Biological Macromolecules. 2024; 279: 134978. https://doi.org/10.1016/j.ijbiomac.2024.134978.

[6] Luo B, Wang S, Song X, Chen S, Qi Q, Chen W, *et al*. An Encapsulation-Free and Hierarchical Porous Triboelectric Scaffold with Dynamic Hydrophilicity for Efficient Cartilage Regeneration. Advanced Materials. 2024; 36: e2401009. https://doi.org/10.1002/adma.202401009.

[7] Xu Y, Guo Y, Li Y, Huo Y, She Y, Li H, *et al*. Biomimetic Trachea Regeneration Using a Modular Ring Strategy Based on Poly(Sebacoyl Diglyceride)/Polycaprolactone for Segmental Trachea Defect Repair. Advanced Functional Materials. 2020; 30: 2004276. https://doi.org/10.1002/adfm.202004276.

[8] Gao E, Wang Y, Wang P, Wang Q, Wei Y, Song D, *et al*. C-Shaped Cartilage Development Using Wharton's Jelly-Derived Hydrogels to Assemble a Highly Biomimetic Neotrachea for use in Circumferential Tracheal Reconstruction. Advanced Functional Materials. 2023; 33: 2212830. https://doi.org/10.1002/adfm.202212830.

[9] Ebihara G, Sato M, Yamato M, Mitani G, Kutsuna T, Nagai T, *et al*. Cartilage repair in transplanted scaffold-free chondrocyte sheets using a minipig model. Biomaterials. 2012; 33: 3846–3851. https://doi.org/10.1016/j.biomaterials.2012.01.056.

[10] Goh CS, Joethy JV, Tan BK, Wong M. Large animal models for long-segment tracheal reconstruction: a systematic review. The Journal of Surgical Research. 2018; 231: 140–153. https://doi.org/10.1016/j.jss.2018.05.025.

[11] Xia D, Jin D, Wang Q, Gao M, Zhang J, Zhang H, *et al*. Tissue-engineered trachea from a 3D-printed scaffold enhances whole-segment tracheal repair in a goat model. Journal of Tissue Engineering and Regenerative Medicine. 2019; 13: 694–703. https://doi.org/10.1002/term.2828.

[12] Li K, Zhu Y, Alini M, Stoddart MJ, Grad S, Li Z. Establishment of a Coculture System with Osteochondral and Synovial Explants as an Ex Vivo Inflammatory Osteoarthritis Model. European Cells & Materials. 2024; 47: 15–29. https://doi.org/10.22203/eCM.v047a02.

[13] Wang B, Fei X, Yin HF, Xu XN, Zhu JJ, Guo ZY, *et al*. Photothermal-Controllable Microneedles with Antitumor, Antioxidant, Angiogenic, and Chondrogenic Activities to Sequential Eliminate Tracheal Neoplasm and Reconstruct Tracheal Cartilage. Small. 2024; 20: e2309454. https://doi.org/10.1002/smll.202309454.

[14] Zeng T, Yuan P, Liang L, Zhang X, Zhang H, Wu W. Cartilaginous Extracellular Matrix Enriched with Human Gingival Mesenchymal Stem Cells Derived "Matrix Bound Extracellular Vesicles" Enabled Functional Reconstruction of Tracheal Defect. Advanced Science. 2022; 9: e2102735. https://doi.org/10.1002/advs.202102735.

[15] Xu Y, Duan H, Li Y, She Y, Zhu J, Zhou G, *et al*. Nanofibrillar Decellularized Wharton's Jelly Matrix for Segmental Tracheal Repair. Advanced Functional Materials. 2020; 30: 1910067. https://doi.org/10.1002/adfm.201910067.

[16] Xu Y, Li D, Yin Z, He A, Lin M, Jiang G, *et al*. Tissue-engineered trachea regeneration using decellularized trachea matrix treated with laser micropore technique. Acta Biomaterialia. 2017; 58: 113–121. https://doi.org/10.1016/j.actbio.2017.05.010.

[17] Xu Y, Dai J, Zhu X, Cao R, Song N, Liu M, *et al*. Biomimetic Trachea Engineering via a Modular Ring Strategy Based on Bone-Marrow Stem Cells and Atelocollagen for Use in Extensive Tracheal Reconstruction. Advanced Materials. 2022; 34: e2106755. https://doi.org/10.1002/adma.202106755.

[18] Yang M, Sun W, Wang L, Tang H, Xu X, Yang L, *et al*. Curcumin loaded polycaprolactone scaffold capable of anti-inflammation to enhance tracheal cartilage regeneration. Materials & Design. 2022; 224: 111299. https://doi.org/10.1016/j.matdes.2022.111299.

[19] Xu S, Zhao S, Jian Y, Shao X, Han D, Zhang F, *et al*. Icariin-loaded hydrogel with concurrent chondrogenesis and anti-inflammatory properties for promoting cartilage regeneration in a large animal model. Frontiers in Cell and Developmental Biology. 2022; 10: 1011260. https://doi.org/10.3389/fcell.2022.1011260.

[20] Liu Y, Li D, Yin Z, Luo X, Liu W, Zhang W, *et al*. Prolonged in vitro precultivation alleviates post-implantation inflammation and promotes stable subcutaneous cartilage formation in a goat model. Biomedical Materials. 2016; 12: 015006. https://doi.org/10.1088/1748-605x/12/1/015006.

[21] Shen Y, Tu T, Yi B, Wang X, Tang H, Liu W, *et al*. Electrospun acid-neutralizing fibers for the amelioration of inflammatory response. Acta Biomaterialia. 2019; 97: 200–215. https://doi.org/10.1016/j.actbio.2019.08.014.

[22] Li D, Yin Z, Liu Y, Feng S, Liu Y, Lu F, *et al*. Regeneration of trachea graft with cartilage support, vascularization, and epithelization. Acta Biomaterialia. 2019; 89: 206–216. https://doi.org/10.1016/j.actbio.2019.03.003.

[23] Takezawa T, Mori Y, Yoshizato K. Cell Culture on a Thermo-Responsive Polymer Surface. Bio/technology. 1990; 8: 854–856. https://doi.org/10.1038/nbt0990-854.

[24] Lu Y, Zhang W, Wang J, Yang G, Yin S, Tang T, *et al*. Recent advances in cell sheet technology for bone and cartilage regeneration: from preparation to application. International Journal of Oral Science. 2019; 11: 17. https://doi.org/10.1038/s41368-019-0050-5.

[25] Dikina AD, Alt DS, Herberg S, McMillan A, Strobel HA, Zheng Z, *et al*. A Modular Strategy to Engineer Complex Tissues and Organs. Advanced Science. 2018; 5: 1700402. https://doi.org/10.1002/advs.201700402.

[26] Sato M, Yamato M, Mitani G, Takagaki T, Hamahashi K, Nakamura Y, *et al*. Combined surgery and chondrocyte cell-sheet transplantation improves clinical and structural outcomes in knee osteoarthritis. NPJ Regenerative Medicine. 2019; 4: 4. https://doi.org/10.1038/s41536-019-0069-4.

[27] Shen Z, Sun F, Shan Y, Lu Y, Wu C, Zhang B, *et al*. Construction of a novel cell-free tracheal scaffold promoting vascularization for repairing tracheal defects. Materials Today. Bio. 2023; 23: 100841. https://doi.org/10.1016/j.mtbio.2023.100841.

[28] Yang M, Chen J, Chen Y, Lin W, Tang H, Fan Z, *et al*. Scaffold-Free Tracheal Engineering via a Modular Strategy Based on Cartilage and Epithelium Sheets. Advanced Healthcare Materials. 2023; 12: e2302076. https://doi.org/10.1002/adhm.202302076.

[29] Martinod E, Chouahnia K, Radu DM, Joudiou P, Uzunhan Y, Bensidhoum M, *et al*. Feasibility of Bioengineered Tracheal and Bronchial Reconstruction Using Stented Aortic Matrices. JAMA. 2018; 319: 2212–2222. https://doi.org/10.1001/jama.2018.4653.

[30] Guinde J, Bismuth J, Laroumagne S, Coiffard B, Astoul P, Thomas

PA, *et al*. Bifurcated Silicone Stents for the Management of Anastomotic Complications in Lung Transplanted Patients: Ten Years' Experience. Respiration; International Review of Thoracic Diseases. 2022; 101: 675–682. https://doi.org/10.1159/000523755.

[31] Sakaguchi Y, Sato T, Muranishi Y, Yutaka Y, Komatsu T, Omori K, *et al*. Development of a novel tissue-engineered nitinol frame artificial trachea with native-like physical characteristics. The Journal of Thoracic and Cardiovascular Surgery. 2018; 156: 1264–1272. https://doi.org/10.1016/j.jtcvs.2018.04.073.

[32] Fabre D, Kolb F, Fadel E, Mercier O, Mussot S, Le Chevalier T, *et al*. Successful Tracheal Replacement in Humans Using Autologous Tissues: An 8-Year Experience. The Annals of Thoracic Surgery. 2013; 96: 1146–1155. https://doi.org/10.1016/j.athoracsur.2013.05.073.

[33] Grillo HC. Tracheal replacement: A critical review. The Annals of Thoracic Surgery. 2002; 73: 1995–2004. https://doi.org/10.1016/S0003-4975(02)03564-6.

[34] Genden EM, Miles BA, Harkin TJ, DeMaria S, Kaufman AJ, Mayland E, *et al*. Single-stage long-segment tracheal transplantation. American Journal of Transplantation: Official Journal of the American Society of Transplantation and the American Society of Transplant Surgeons. 2021; 21: 3421–3427. https://doi.org/10.1111/ajt.16752.

[35] Hamilton NJ, Kanani M, Roebuck DJ, Hewitt RJ, Cetto R, Culme-Seymour EJ, *et al*. Tissue-Engineered Tracheal Replacement in a Child: A 4-Year Follow-Up Study. American Journal of Transplantation: Official Journal of the American Society of Transplantation and the American Society of Transplant Surgeons. 2015; 15: 2750–2757. https://doi.org/10.1111/ajt.13318.

[36] Delaere PR, Vranckx JJ, Den Hondt M; Leuven Tracheal Transplant Group. Tracheal Allograft after Withdrawal of Immunosuppressive Therapy. The New England Journal of Medicine. 2014; 370: 1568–1570. https://doi.org/10.1056/NEJMc1315273.

[37] Weber JF, Rehmani SS, Baig MZ, Jadoon Y, Bhora FY. Successes and Failures in Tracheal Bioengineering: Lessons Learned. The Annals of Thoracic Surgery. 2021; 112: 1089–1094. https://doi.org/10.1016/j.athoracsur.2020.10.021.

[38] Furlow PW, Mathisen DJ. Surgical anatomy of the trachea. Annals of Cardiothoracic Surgery. 2018; 7: 255–260. https://doi.org/10.21037/acs.2018.03.01.

[39] Delaere P, Van Raemdonck D, Vranckx J. Tracheal transplantation. Intensive Care Medicine. 2019; 45: 391–393. https://doi.org/10.1007/s00134-018-5445-9.

[40] Makris D, Holder-Espinasse M, Wurtz A, Seguin A, Hubert T, Jaillard S, *et al*. Tracheal Replacement With Cryopreserved Allogenic Aorta. Chest. 2010; 137: 60–67. https://doi.org/10.1378/chest.09-1275.

[41] Delaere P, Vranckx J, Verleden G, De Leyn P, Van Raemdonck D; Leuven Tracheal Transplant Group. Tracheal Allotransplantation after Withdrawal of Immunosuppressive Therapy. The New England Journal of Medicine. 2010; 362: 138–145. https://doi.org/10.1056/NEJMoa0810653.

[42] Sykes M. Immune Evasion by Chimeric Trachea. The New England Journal of Medicine. 2010; 362: 172–174. https://doi.org/10.1056/NEJMe0908366.

[43] Hysi I, Wurtz A, Zawadzki C, Kipnis E, Jashari R, Hubert T, *et al*. Immune tolerance of epithelium-denuded-cryopreserved tracheal allograft. European Journal of Cardio-thoracic Surgery: Official Journal of the European Association for Cardio-thoracic Surgery. 2014; 45: e180–e186. https://doi.org/10.1093/ejcts/ezu133.

[44] De Wolf J, Brieu M, Zawadzki C, Ung A, Kipnis E, Jashari R, *et al*. Successful immunosuppressant-free heterotopic transplantation of tracheal allografts in the pig. European Journal of Cardio-thoracic Surgery: Official Journal of the European Association for Cardio-thoracic Surgery. 2017; 52: 248–255. https://doi.org/10.1093/ejcts/ezx116.

[45] Bae SW, Lee KW, Park JH, Lee J, Jung CR, Yu J, *et al*. 3D Bioprinted Artificial Trachea with Epithelial Cells and Chondrogenic-Differentiated Bone Marrow-Derived Mesenchymal Stem Cells. International Journal of Molecular Sciences. 2018; 19: 1624. https://doi.org/10.3390/ijms19061624.

[46] Pang Q, Chen Z, Li X, Zhan J, Huang W, Lei Y, *et al*. Cytokine-Activated Mesenchymal-Stem-Cell-Derived Extracellular Matrix Facilitates Cartilage Repair by Enhancing Chondrocyte Homeostasis and Chondrogenesis of Recruited Stem Cells. Research: A Science Partner Journal. 2025; 8: 0700. https://doi.org/10.34133/research.0700.

[47] Takahashi H, Okano T. Thermally-triggered fabrication of cell sheets for tissue engineering and regenerative medicine. Advanced Drug Delivery Reviews. 2019; 138: 276–292. https://doi.org/10.1016/j.addr.2019.01.004.

[48] Ortiz-Comino RM, Morales A, López-Lisbona R, Cubero N, Diez-Ferrer M, Tebé C, *et al*. Silicone Stent Versus Fully Covered Metallic Stent in Malignant Central Airway Stenosis. The Annals of Thoracic Surgery. 2021; 111: 283–289. https://doi.org/10.1016/j.athoracsur.2020.04.141.

[49] Li L, Zhang X, Shi J, Chen Y, Wan H, Herth FJ, *et al*. Airway Stents from Now to the Future: A Narrative Review. Respiration; International Review of Thoracic Diseases. 2023; 102: 439–448. https://doi.org/10.1159/000530421.

Editor's note: The Scientific Editors responsible for this paper were Matteo D' Este and Martin Stoddart.

Received: 8th August 2025; **Accepted**: 12th May 2026; **Published**: 26th June 2026